Molecular Therapy
Methods & Clinical Development
Original Article

AAV vectors engineered to target insulin receptor greatly enhance intramuscular gene delivery

Cody B. Jackson,[1] Audrey S. Richard,[1,4] Amrita Ojha,[1] Kimberly A. Conkright,[2] Jeffrey M. Trimarchi,[2] Charles C. Bailey,[2] Michael D. Alpert,[2] Mark A. Kay,[3] Michael Farzan,[1] and Hyeryun Choe[1]

[1]Department of Immunology and Microbiology, The Scripps Research Institute, 130 Scripps Way, Jupiter, FL 33458, USA; [2]Emmune, Inc., 14155 US Highway 1, Juno Beach, FL 33408, USA; [3]Departments of Pediatrics and Genetics, Stanford University, 269 Campus Dr. Rm 2105, Stanford, CA 94305, USA

Adeno-associated virus (AAV) is one of the most commonly used vectors for gene therapy, and the applications for AAV-delivered therapies are numerous. However, the current state of technology is limited by the low efficiency with which most AAV vectors transduce skeletal muscle tissue. We demonstrate that vector efficiency can be enhanced by modifying the AAV capsid with a peptide that binds a receptor highly expressed in muscle tissue. When an insulin-mimetic peptide, S519, previously characterized for its high affinity to insulin receptor (IR), was inserted into the capsid, the AAV9 transduction efficiency of IR-expressing cell lines as well as differentiated primary human muscle cells was dramatically enhanced. This vector also exhibited efficient transduction of mouse muscle *in vivo*, resulting in up to 18-fold enhancement over AAV9. Owing to its superior transduction efficiency in skeletal muscle, we named this vector "enhanced AAV9" (eAAV9). We also found that the modification enhanced the transduction efficiency of several other AAV serotypes. Together, these data show that AAV transduction of skeletal muscle can be improved by targeting IR. They also show the broad utility of this modular strategy and suggest that it could also be applied to next-generation vectors that have yet to be engineered.

INTRODUCTION

Recombinant adeno-associated virus (AAV) vectors are widely considered to be the gold standard for gene therapy, owing to their safety, persistence of gene expression, and decades of extensive study. There have been several recent successes in treating human diseases with AAV-expressed transgenes,[1] including regulatory approvals of an AAV2-based gene replacement therapy for RPE65-mediated congenital blindness[2] and an AAV9-based gene replacement therapy for spinal muscular atrophy,[3] as well as a number of successful phase II and III trials for hemophilia A and B using natural and bio-engineered capsids.[4,5] However, there are several challenges associated with using AAV to express therapeutic transgenes, especially at high concentrations. First, the high cost of AAV production precludes its widespread use in the developing world.[6] Second, the AAV vector's capsid and DNA trigger innate immune responses, and higher levels of anti-drug antibodies are elicited by expression of a therapeutic protein from muscle than with the passive infusion of a protein.[6–9] Third, practical constraints on AAV concentrations and injection volumes limit the magnitude of transgene expression.[10–12] Most of these challenges could be eased with the development of more efficient vectors.

Skeletal muscle is an excellent target tissue for gene delivery because direct injection into skeletal muscle is clinically convenient and transgenes expressed therein can freely diffuse into systemic circulation.[13,14] Transduction of skeletal muscle also has other distinct advantages in safety, persistence, and efficacy. Local muscle inflammation does not lead to major clinical complications, such as metabolic perturbations, which may be elicited by transduction of the liver. Additionally, terminally differentiated muscle cells are longer lived than many other cell types and do not divide, although turnover will occur over time with injury or immune response. Therefore, transgene expression in skeletal muscle lasts for years or even decades.[14,15] Finally, vectors encounter less preexisting anti-capsid antibodies when injected intramuscularly, an important advantage for treatment of AAV-seropositive individuals or repeated treatments.[16] However, a major caveat of muscle transduction is that it may elicit more anti-transgene antibodies than the liver.[17] Lower doses and less immunogenic capsids, promoters, and transgenes may help overcome this problem.

A wealth of research has focused on improving the transduction efficiency or modifying the tropism of AAV capsids, either by rational design[18] or through a range of directed evolution approaches, including capsid shuffling, random panning mutagenesis, and peptide library display.[19,20] Both approaches offer the opportunity to retarget

Received 8 July 2020; accepted 11 November 2020;
https://doi.org/10.1016/j.omtm.2020.11.004.

[4]Present address: European Research Infrastructure on Highly Pathogenic Agents, 101 Rue de Tolbiac, 75013 Paris, France

Correspondence: Hyeryun Choe, Department of Immunology and Microbiology, The Scripps Research Institute, 130 Scripps Way #2B2, Jupiter, FL 33458, USA.
E-mail: hchoe@scripps.edu

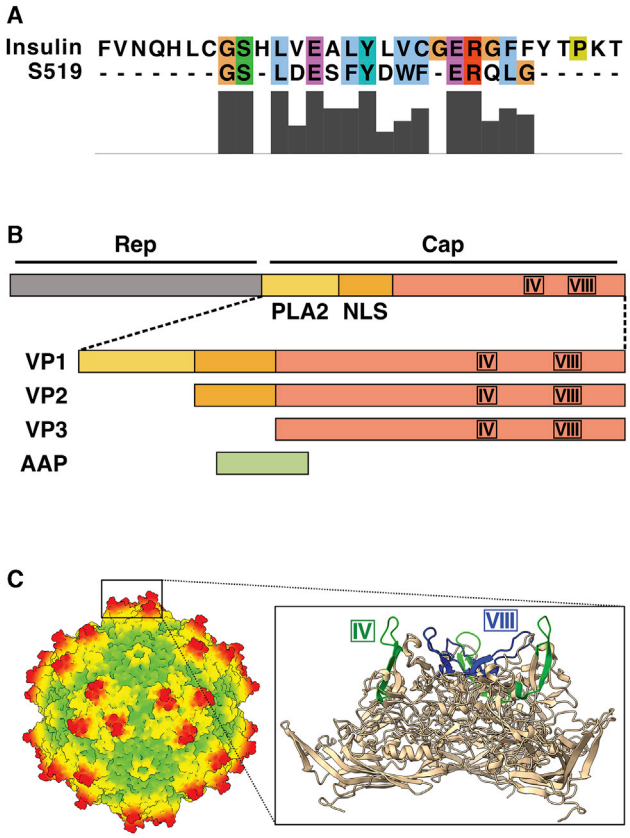

Figure 1. Insulin mimetic peptide S519 and its insertion into the AAV9 capsid

(A) A segment of the S519 peptide was aligned to the human insulin B chain using the MUSCLE algorithm and visualized in JalView;[38,39] amino acid similarity is plotted below the alignment. (B) A diagram of the AAV genome shows the assembly activating protein (AAP) and three VP proteins translated from a single Cap gene; VP1, VP2, and VP3. All display the same C-terminal region and thus all contain variable regions IV and VIII (VR-IV and VR-VIII). (C) The AAV9 cryo-EM structure (PDB: 3UX1) was visualized with ChimeraX software.[40] Virion surface is colored by distance from the center of the virion. In the expanded view of the threefold axis of symmetry, VR-IV and VR-VIII are colored in green and blue, respectively.

or enhance AAV transduction of a specific target cell. On one hand, when a novel AAV capsid is created by directed evolution, the acquired phenotype is often serotype-specific and mechanistic insight is hard to gain. On the other hand, a rational design approach can allow greater mechanistic insight and control over the phenotype, but often does not result in the desired effect when tested *in vivo*. Because of technical advances such as automated DNA synthesis and next generation sequencing, many recent advances in AAV vector engineering have come from directed evolution campaigns. Recent examples include capsid variants targeted to cell types in the brain,[21–23] cochlea,[24] and retina.[25,26] An example of an effective rational design was shown by targeting three distinct cellular receptors using antibody-antigen interaction following the genetic fusion of nanobodies into AAV capsids.[27] In another example, mutation of tyrosine residues on the AAV capsid has been shown to enhance transduction by avoiding proteasomal degradation in several combinations of serotypes and target tissues.[28–30] In all modalities, however, translatability has been a challenge. For example, a vector may perform well in a cell line but not *in vivo*, or it may be successful in murine but not in human cells.

In this study, using the well-established method of peptide insertion into the capsid,[19] we developed a system that not only markedly improves vector efficiency in skeletal muscle transduction but also is portable to other AAV serotypes. In addition, because the peptide binds murine and human receptors alike, results derived from animal studies are likely translatable to humans. To develop this system, we first identified receptors that are abundantly expressed on skeletal muscle cells and then short ligands that bind these receptors with high affinity and that have already been characterized. We found that insulin receptor (IR) is expressed in abundance on differentiated skeletal muscle cells and has a synthetic ligand of suitable length and high affinity.[31] We genetically grafted this ligand into the capsid of AAV9 and several other serotypes in variable regions IV or VIII (VR-IV or VR-VIII), which were well established to be amenable to insertion of foreign sequences.[19,32–37] We show that the vectors modified with this insert have greatly enhanced transduction efficiency in IR-expressing cell lines, primary human myotubes, and mouse skeletal muscle *in vivo* compared to their parental counterparts. Further, we demonstrate that their enhanced transduction efficiency is transferable to other natural serotypes and engineered AAV vectors. Collectively, these data indicate that targeting a specific receptor using a well-characterized ligand is a valuable strategy because it not only improves vector efficiency but also is portable to other vectors.

RESULTS

Modification of AAV9 with the insulin-mimetic peptide S519 facilitates enhanced transduction of IR-expressing cells

The insulin-mimetic peptide S519 is a 36 amino acid linear peptide with a K_D for IR of 2.0×10^{-11} M.[31] This peptide is an IR agonist[31] and shows sequence similarity with human insulin (Figure 1A). We cloned a coding sequence for this peptide into VR-IV and VR-VIII of the AAV9 capsid. Because VP1, VP2, and VP3 are translated from one gene, all three VP molecules carry the insert (Figure 1B). The cryo-electon microscopy (cryo-EM) structure of AAV9 reveals that VR-IV and VR-VIII protrude furthest from the virion among all surface-exposed residues[41] (Figure 1C). We chose to insert S519 between residues near the apex of each loop, after G543 for VR-IV or A589 for VR-VIII (by AAV9 residue numbering) with a short linker (Table S1).

Because VR-IV and VR-VIII are located at the threefold axis of symmetry and there are three copies each of VR-IV and VR-VIII per threefold axis, we hypothesized that vector production with the relatively large insert may be hampered by steric hindrance. Therefore, we reduced steric hindrance by mixing wild-type (WT) and S519-containing mutant capsids during vector production and assessed the mosaic vectors' yield and infectivity. We found that transfection with less mutant than WT capsid (at ratios between 20:1 and 3:1 of WT to mutant) resulted in greater yields compared to a higher mutant

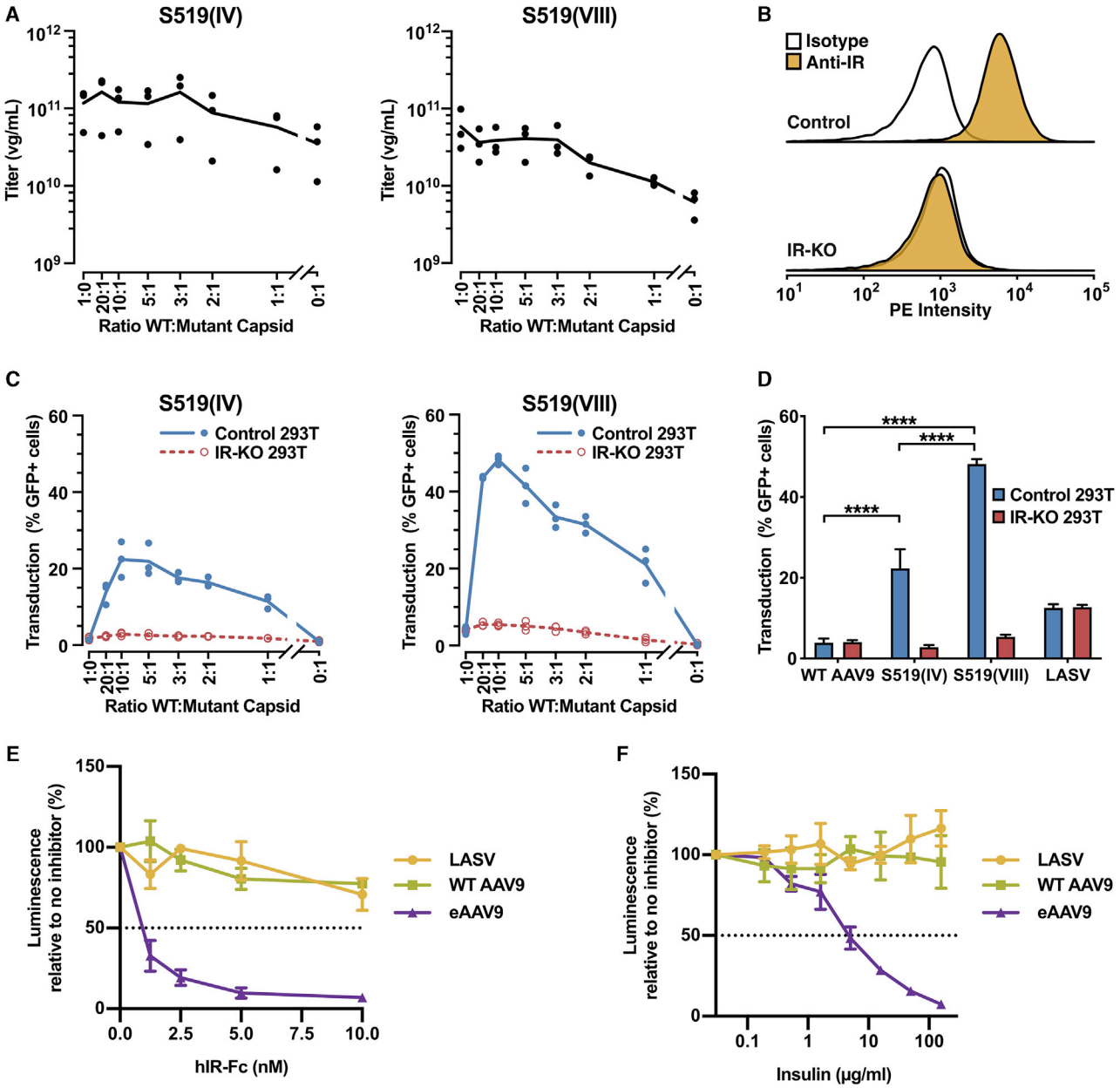

Figure 2. Insertion of the insulin-mimetic peptide S519 into the capsid markedly enhances AAV9 transduction efficiency *in vitro*

(A) Mosaic vectors were produced with the indicated ratios of WT to S519(IV) or S519(VIII) Rep/Cap plasmid. Vectors were quantified by qPCR. Each dot represents the vector titer from one experiment, and trend lines represent the mean of three independent experiments. (B) HEK293T cells transduced with CRISPR-Cas9 and untargeted guide RNA (Control 293T) or guide RNA directed against IR (IR-KO 293T) were analyzed for IR expression by flow cytometry. Representative data from three independent experiments are shown. (C) GFP-encoding mosaic vectors produced with the indicated ratios were used to transduce cells at an MOI of 10^5 vg/cell. GFP expression was measured by flow cytometry after 24 h. Trend lines are the mean of three independent experiments. (D) Cells were transduced with the indicated vector at an MOI of 10^5 vg/cell or a comparable quantity of LASV pseudovirus. S519(IV)-AAV9 and S519(VIII)-AAV9 were produced as mosaic vectors at a 10:1 ratio of WT to mutant capsid. GFP expression was analyzed 24 h post transduction (hpt). Data are shown as mean ± SEM of three independent experiments, and statistical significance was assessed by two-way ANOVA with Tukey's multiple comparisons test (****$p < 0.0001$). (E) The indicated concentrations of IR-Fc were incubated with firefly luciferase (FLuc)-encoding vectors for 15 minutes before addition to HEK293T cells for 60-minute transduction. Luciferase activity was measured 24 hpt. Data are shown as mean ± SEM of 3 independent experiments. (F) HEK293T cells were preincubated with the indicated concentrations of insulin for 15 minutes, and FLuc-encoding vectors were added to the culture for 60 min. Luciferase activity was measured 24 hpt. Data are shown as mean ± SEM of three independent experiments.

capsid ratio, and their titers were comparable to that of WT AAV9 (Figure 2A). This was true for both the vectors modified at either VR-IV or VR-VIII (S519(IV)-AAV9 or S519(VIII)-AAV9, respectively). To compare transduction efficiency of these mosaic vectors, we generated IR-knockout HEK293T cells (IR-KO 293T) using the LentiCRISPRv2 system[42] (Figure 2B). We also generated cells transduced with a single guide RNA (sgRNA) with no human genomic target but treated in the same way as IR-KO cells (control 293T). Control 293T cells maintain endogenous IR expression. We transduced both these cells with the same mosaic vectors, which express green fluorescent protein (GFP) under human cytomegalovirus (CMV) promoter, at a multiplicity of infection (MOI) of 10^5 vector genomes (vg) per cell and analyzed GFP expression by flow cytometry at 24 h post transduction (Figure 2C). We found that vectors produced with a 10:1 ratio of WT to mutant capsid yielded the highest expression of the GFP reporter in control 293T cells, while transduction of IR-KO 293T was much lower for all mosaic vectors. Therefore, we chose to use a 10:1 ratio for the study. These data show that there is an optimum number of mutant capsids that can be accommodated by a virion and warrant future study to identify the actual ratio of WT and mutant capsids incorporated into a mature virion. These data also suggest a balance between maximizing mutant capsids per virion to enhance transduction and minimizing physical constraints caused by the mutant capsids present in the threefold axis.

Next, we compared S519(IV)- and S519(VIII)-AAV9 side-by-side with WT AAV9 for their transduction efficiency in the IR-KO and control 293T cells. A retrovirus pseudotyped with the entry protein of Lassa fever virus (LASV) was used as a control because its transduction is not dependent on the presence of IR. We observed that, while both S519(IV)- and S519(VIII)-AAV9 transduced IR-KO cells with low efficiency, they transduced control 293T cells with greater efficiency than WT AAV9 and that transduction efficiency of S519(VIII)-AAV9 was substantially higher than S519(IV)-AAV9 (Figure 2D). Lower levels of transduction of IR-KO cells is specific to our IR-directed vectors and not due to perturbation in those cells because WT AAV9 and LASV pseudovirus have similar reporter expression in both the IR-KO and control 293T cells. Similar to the enhanced reporter expression mediated by GFP-encoding S519(VIII)-AAV9 in control 293T cells, this effect was also reproduced with firefly luciferase (FLuc)-encoding vectors (Figure S1A). Because of the superior transduction efficiency of S519(VIII)-AAV9, we hereafter refer to this vector as "enhanced AAV9" (eAAV9).

To verify IR-dependence of eAAV9, we used a construct consisting of the human IR ectodomain fused to an Fc tag (IR-Fc)[43] as a transduction inhibitor. Control 293T cells were transduced with FLuc-encoding WT AAV9, eAAV9, or LASV psudovirus alone or together, with increasing concentrations of IR-Fc protein, and analyzed for luciferase activity 24 h later. Preincubation of eAAV9 with IR-Fc induced a dose-dependent decrease in transduction of HEK293T cells half maximal inhibitory concentration (IC_{50}), 0.60 nM), while WT AAV9 and LASV were unaffected (Figure 2E). Similarly, we also evaluated insulin for its inhibitory effect on transduction by WT AAV9 and eAAV9 and found that preincubation of vectors with human insulin exhibited dose-dependent inhibition of eAAV9 ($IC_{50,}$ 5.2 μg/ml) but not WT AAV9 (Figure 2F). Further, to confirm that the enhanced reporter gene expression is a consequence of increased vector entry, we quantified intracellular vector genomes in transduced cells (Figure S1B). Consistent with the observed differences in reporter gene expression, we found that transduction with eAAV9 compared to WT AAV9 results in a substantially increased intracellular vector genome copy number in control 293T cells, but not in IR-KO 293T cells. The cycle threshold (Ct) of a qPCR assay targeting the human housekeeping gene *GAPDH* was similar in all conditions, indicating that the observed differences in intracellular vg copy number are not due to discrepancies in genomic DNA extraction. These data clearly show that eAAV9 transduces HEK293T cells with much greater efficiency than WT AAV9 and that this enhanced transduction is mediated by its use of IR.

eAAV9 transduces human myotubes much more efficiently than WT AAV9 in an IR-dependent manner

We next sought to determine whether this capsid modification was effective in human skeletal muscle cells. Cells isolated from the rectus abdominis muscle of healthy donors were cultured and differentiated to form myotubes and transduced with 7×10^{10} vg of GFP-expressing WT AAV9 or eAAV9 per square centimeter of culture area with or without addition of the IR-Fc inhibitor. LASV pseudovirus was used as a control. Three days later, the cells were visualized by fluorescent microscopy. Cells transduced with eAAV9 showed greatly enhanced GFP expression compared to those transduced with WT AAV9 (Figure 3). At this MOI, WT AAV9 was scarcely distinguishable from mock-transduced cells in GFP imaging. Preincubation of eAAV9 with 30 nM IR-Fc greatly reduced its transduction, confirming that the enhanced efficiency of this vector is derived from its use of IR. IR-Fc had no effect on LASV, which enters through α-dystroglycan.[44] To verify that the overall population of cells in each condition was similar, we also visualized nuclei by Hoechst 33342 staining and took advantage of cellular autofluorescence (primarily due to intracellular porphyrin compounds) to visualize the cell density and morphology as previously described.[45,46] Of note, cells exposed to LASV exhibited cytopathic effects, resulting in cell detachment. The remaining GFP-expressing cells were of a distinct stellate morphology, suggesting that myotubes were either not transduced by LASV pseudovirus or nonviable after transduction. On the other hand, eAAV9-transduced cells exhibited no cytopathic effects and the transduced cells were of elongated tubular morphology, demonstrating that eAAV9 preferentially transduces differentiated myotubes.

eAAV9 transduces mouse skeletal muscle *in vivo* more efficiently than WT AAV9 and its efficiency is further enhanced by fasting.

Because mouse IR (mIR) is 94% identical to human IR in amino-acid sequence, we hypothesized that eAAV9 would exhibit enhanced transduction in mIR-expressing cells too. To confirm this, we acquired two mouse brown preadipocyte cell lines: one with IR and

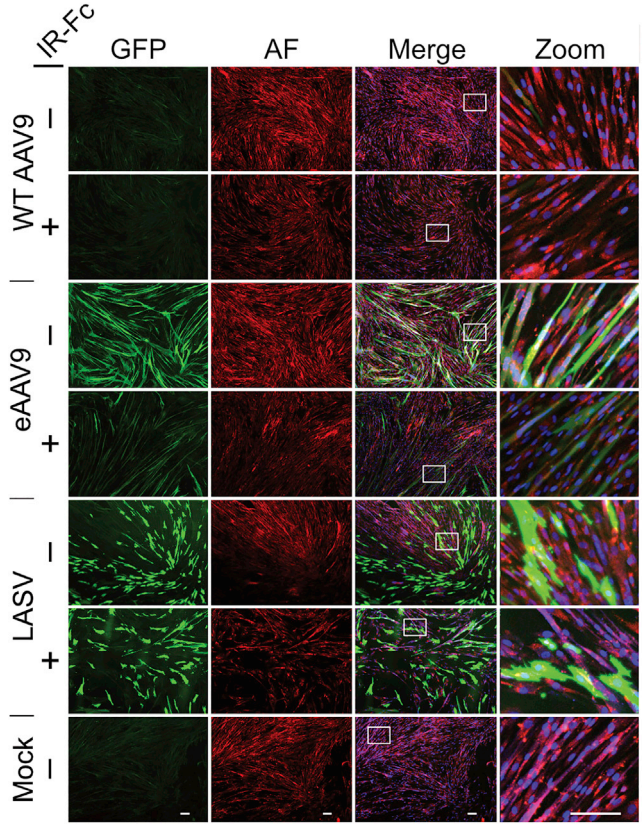

Figure 3. eAAV9 is markedly more efficient in transducing primary human skeletal muscle cells compared to WT AAV9

Primary human skeletal muscle cells were differentiated to form myotubes and transduced with the indicated vectors expressing GFP that were preincubated or not with 30 nM IR-Fc. After 3 days of culture in growth media, cells were fixed and stained with Hoechst 33342 to label nuclei. Green, GFP reporter; red, cellular autofluorescence for morphology visualization; blue (included in Merge), Hoechst 33342. Scale bar (bottom panels) represents 100 μm. Representative images are shown from one of 3 independent experiments with cells sourced from 2 different donors.

insulin-like growth factor I receptor double knockout (DKO) and a derivative of the same that was reconstituted with mIR (DKO+mIR).[47] We transduced both cells with GFP-expressing WT AAV9 and eAAV9. In contrast to WT AAV9, which yielded modest GFP expression in DKO and DKO+mIR cells, transduction with eAAV9 resulted in robust expression of GFP only in the DKO+mIR cells (Figure S2).

As eAAV9 efficiently uses mIR, we next determined whether eAAV9 could transduce skeletal muscle of mice more efficiently than WT AAV9 when delivered by intramuscular (i.m.) injection. We injected the gastrocnemius muscles of 11-week-old BALB/c mice with 10^9 vg of luciferase-encoding WT AAV9 or eAAV9. At 14, 21, and 28 days post transduction (dpt), mice were injected with D-luciferin and imaged to measure luciferase activity (Figure 4A). In these experimental conditions, mice injected with eAAV9 exhibited approximately 6-fold greater luciferase activity compared to those injected with WT AAV9.

Because eAAV9 is IR-dependent and because the addition of insulin to the cell culture media had a blocking effect *in vitro* (Figure 2F), we next asked whether transduction *in vivo* would be modulated by the concentration of circulating insulin in the mice. Insulin secretion occurs as a homeostatic process when blood glucose is in excess, e.g., after food consumption.[48,49] Therefore, we evaluated the transduction efficiency of WT AAV9 and eAAV9 in mice that were fasted for 4 h before and after injection of the vectors. As above, mice were injected with 10^9 vg into the gastrocnemius muscle and luciferase activity was measured by bioluminescent imaging (Figure 4B). In fasted mice, eAAV9 yielded approximately 18-fold greater luciferase activity than WT AAV9 at 14, 21, and 28 dpt. We conclude that eAAV9 transduces mouse skeletal muscle *in vivo* with greater efficiency than WT AAV9 and that this phenotype is further enhanced by fasting.

eAAV9 does not perturb glucose homeostasis or differentially transduce extramuscular tissues compared to WT AAV9

Because of the physiological role of insulin in modulating blood glucose levels, we asked whether eAAV9, with its insulin-mimetic insertion, would exert a measurable effect on the blood glucose concentration in mice. Mice were fasted as described above and blood glucose was measured by microsampling immediately before injection of vectors to obtain a baseline value. Mice were injected in the gastrocnemius muscle with 10^9 vg of WT AAV9, eAAV9, or, as a positive control, human insulin at 0.5 U/kg, a typical therapeutic dose for a patient with diabetes mellitus type 2 (Figure 4C). Blood glucose was then measured at 45 min, 2 h, and 4 h post injection of vectors or insulin. Injection of insulin caused a sharp and statistically significant decrease in blood glucose at 45 min as well as a rebound effect at 2 and 4 hours, consistent with its physiological role. On the other hand, blood glucose levels of mice injected with eAAV9 did not significantly differ from those injected with WT AAV9 at any measured time point. We therefore conclude that i.m. administration of eAAV does not perturb systemic glucose homeostasis.

Next, although we engineered eAAV9 for enhanced transduction of muscle when delivered by i.m. injection, we sought to determine if eAAV9 additionally exhibits enhanced systemic transduction compared to WT AAV9 when injected intravenously (i.v.). We also aimed to investigate whether eAAV9 compared to WT AAV9 accumulates at high levels in certain organs, which might lead to toxicity. To obtain a detectable level of luciferase signal, we first titered an optimal amount of vectors for systemic delivery and decided on 10^{11} vg per mouse. Following i.v. injection of 10^{11} vg of luciferase-encoding vector into the tail vein of fasted mice, we observed no significant difference in overall luminescence intensity or in the pattern of tissues transduced by eAAV9 versus WT AAV9 (Figure S3A). As a control, 10^9 vg of the same vector preps were injected into the gastrocnemius muscle of mice handled in parallel and imaged identically. Consistent with other experiments, eAAV9 exhibited roughly 20-fold greater transduction than WT AAV9 with i.m. injection

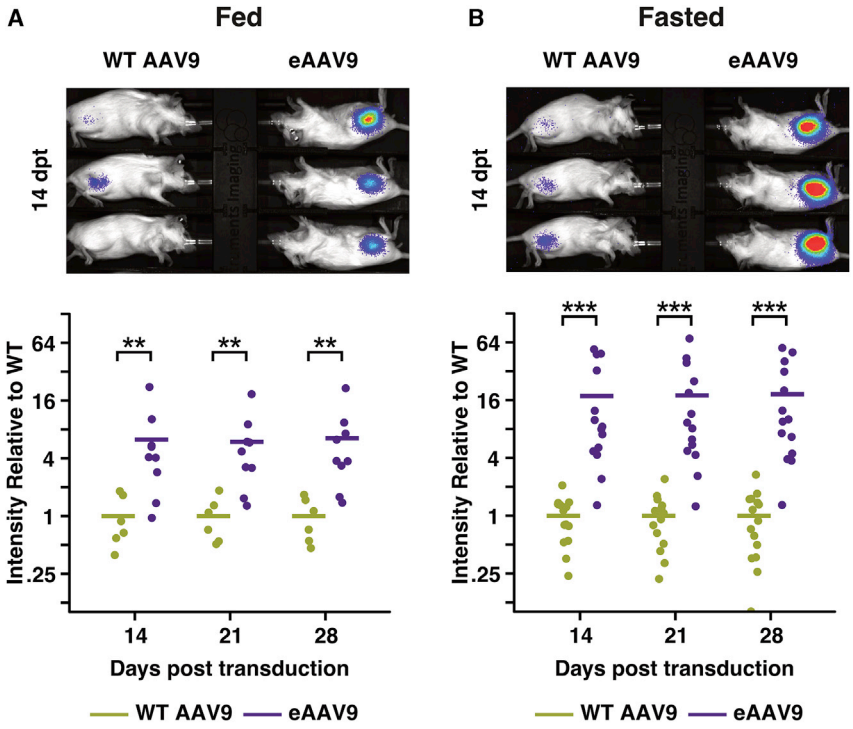

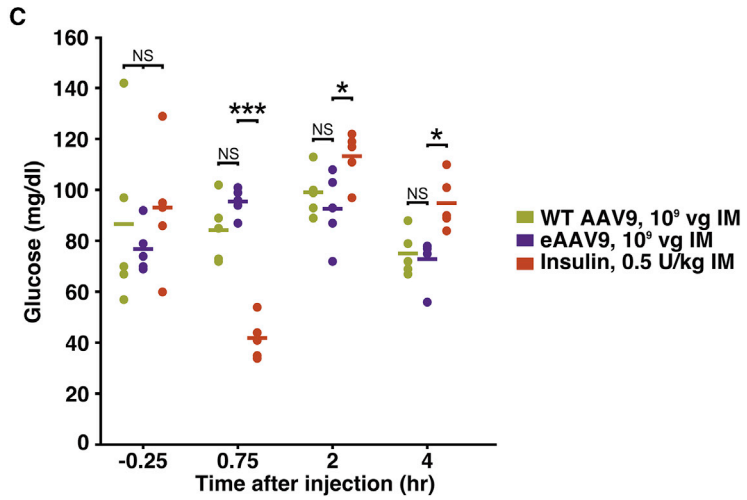

Figure 4. eAAV9 transduces mouse skeletal muscle *in vivo* with much greater efficiency than WT AAV9

(A and B) Mice with *ad libitum* access to food (A, Fed) or fasted for 4 h before and 4 h after transduction (B, Fasted) were injected with 10^9 vg of luciferase-expressing WT AAV9 or eAAV9 vector in the gastrocnemius muscle of the right hindleg and imaged at the indicated time points. Top, representative images of mice at 14 dpt. Bottom, quantification of luminescence; dots represent individual mice and horizontal bars indicate mean values. Data are derived from experiments performed with two independent vector preparations (A, n = 6–9 mice per condition; B, n = 14–15 mice per condition). Statistical significance was analyzed by Mann-Whitney U-test (**$p < 0.01$; ***$p < 0.001$). Transduction efficiency of eAAV9 relative to WT AAV9: (A) 6.3-, 5.9-, and 6.5-fold enhancement for 14, 21, and 28 dpi, respectively; (B) 17.6-, 17.9-, and 18.4-fold enhancement for 14, 21, and 28 dpi, respectively. (C) Mice were fasted for 4 h, and blood glucose was measured before (−0.25 h) and at the indicated times after the injection of AAV9, eAAV9, or 0.5 U/kg human insulin. Representative data from three independent experiments are shown; dots represent individual mice and horizontal bars indicate mean values. Statistical significance among the groups (n = 5 mice per group) was analyzed by two-way ANOVA with Tukey's multiple comparisons test (*$p < 0.05$; ***$p < 0.001$).

(Figure S3B). The i.v.-injected mice were euthanized at 30 dpt and intracellular vector genomes were quantified by qPCR (Figure S3C). Surprisingly, many samples amplified below the limit of detection. Nonetheless, similar to our observations with bioluminescent imaging, the vector copy number in spleen, liver, brain, skeletal muscle, and heart did not significantly differ among mice transduced with WT AAV9 versus eAAV9. Together, the bioluminescent imaging and genome quantification results highlight two points. First, eAAV9 is no more efficient than WT AAV9 when delivered systemically. This may reflect either lower IR expression or higher AAV9 receptor (e.g., galactose) expression in other tissues compared to skeletal muscle. Second, the lack of a significant difference in tissue distribution between WT AAV9 and eAAV9 implies that the insulin mimetic peptide does not significantly modulate extramuscular transduction. This indicates a small quantity of eAAV9 vector that may escape the muscle tissue during delivery will not transduce off-target organs with greater efficiency than a similar quantity of WT AAV9. These results also demonstrate that the advantage of eAAV9 is confined to muscle-specific transduction, but the advantage it confers increases the appeal of muscle targeting for expression of therapeutic transgenes.

Transduction by a wide range of AAV serotypes can be enhanced by the S519 peptide

We then tested whether or not our approach is portable to other serotypes. To do so, we grafted the S519 peptide into similar sites at the apex of VR-VIII in the capsids of natural isolates AAV1, AAV2, and AAV8 as well as the chimeric vector NP22 (Table S1). We chose to include the NP22 capsid because it was selected for improved skeletal muscle transduction.[50] Luciferase-encoding vectors were produced for each serotype at a ratio of 10:1 WT to mutant capsid and used to transduce control 293T and IR-KO 293T cells (Figure 5A). We found that eAAV1 and eAAV8 yielded much higher reporter gene expression than their WT counterparts in control 293T cells, but

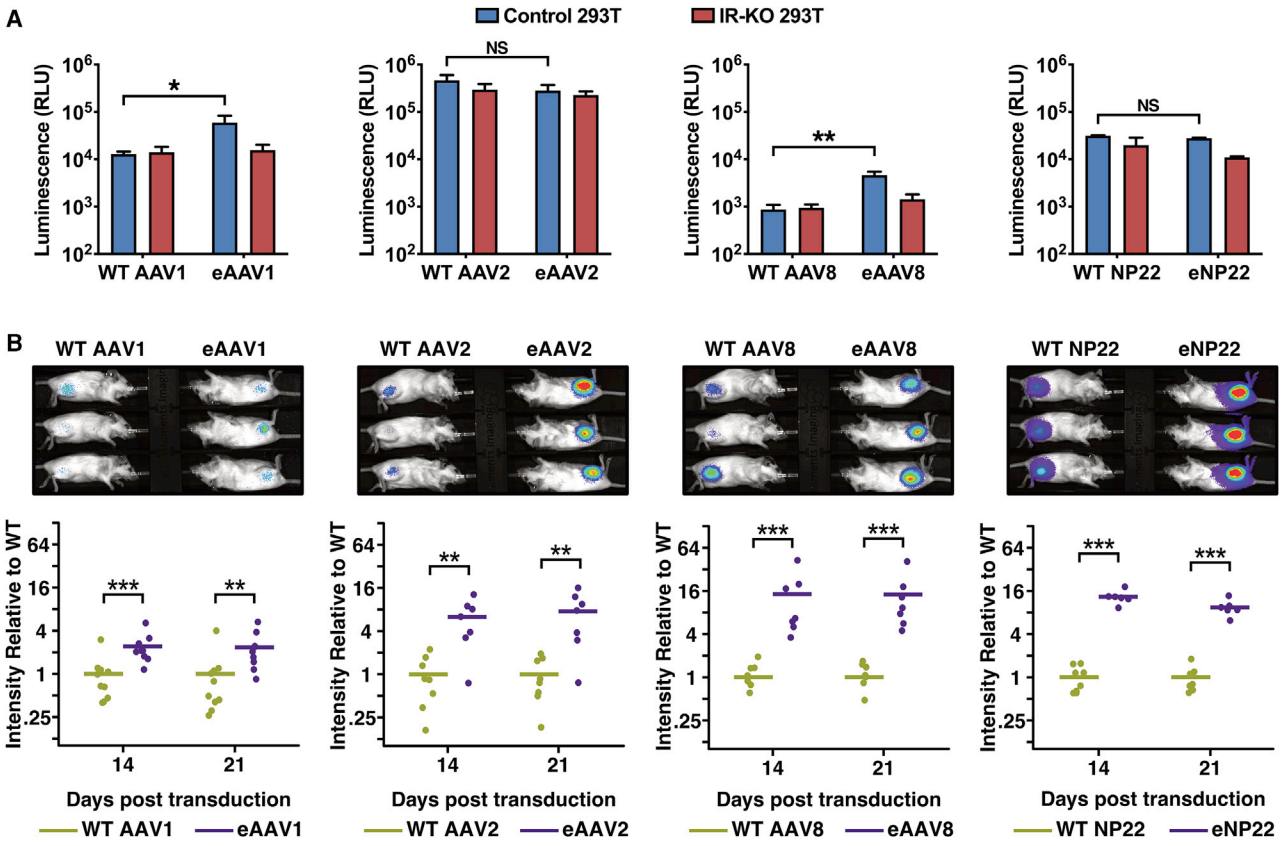

Figure 5. Insertion of the S519 peptide into the capsid enhances the transduction efficiency of a wide range of AAV serotypes

(A) Control 293T or IR-KO 293T cells were transduced with WT or S519-modified vector of the indicated serotypes, encoding luciferase. Luciferase activity was measured 24 hpt. Data are shown as mean ± SEM of three independent experiments, and statistical significance was analyzed by Student's t test (*$p < 0.05$; **$p < 0.01$). (B) Fasted mice were injected in the gastrocnemius muscle with 10^9 vg of WT or S519-modified vector of the indicated serotypes, expressing luciferase, and imaged at 14 and 21 dpt. Top, representative images of mice at 14 dpt. Bottom, quantification of luminescence; dots represent individual mice and horizontal bars indicate mean values. Data are derived from experiments performed with two independent vector preparations (AAV1, n = 9–10 mice per condition; all others, n = 6–8 mice per condition). Statistical significance was analyzed by Mann-Whitney U-test (**$p < 0.01$; ***$p < 0.001$). Transduction efficiency of eAAV relative to parental AAV for 14 and 21 dpt, respectively: 2.4- and 2.4-fold (AAV1), 6.3- and 7.6-fold (AAV2), 14.5- and 14.2-fold (AAV8), and 13.2- and 9.4-fold (NP22).

not in IR-KO 293T cells, confirming that the enhancement of these serotypes is also IR-dependent. In contrast, eAAV2 and eNP22 were indistinguishable from the parental AAV2 and NP22, respectively, in both cell types. Next, we transduced fasted mice by injection of 10^9 vg into the gastrocnemius muscle, and luciferase activity was analyzed by imaging at 14 and 21 dpt (Figure 5B). We included AAV2 and NP22 in the *in vivo* experiments because AAV vectors often behave differently between *in vitro* and *in vivo* transduction. In contrast to our findings in HEK293T cells, eAAV1, eAAV2, eAAV8, and eNP22 all outperformed their WT counterparts in mice. These data show that *in vivo* transduction of skeletal muscle by AAV vectors other than AAV9 is also enhanced when modified by the insertion of the S519 peptide.

DISCUSSION

Steady advances in the field of AAV-mediated gene therapy have made recombinant AAV vectors an increasingly practical choice for gene delivery in a multitude of therapeutic settings. One challenge that remains for many applications is the high doses required to reach effective levels of transgene expression. For example, long-term expression of a monoclonal antibody at levels sufficient for a therapeutic serum concentration was achieved in a rhesus macaque with intramuscular administration of 2.9×10^{12} vg/kg of AAV1.[15] An equivalent dose for an adult human would be on the order of 10^{14} vg, a prohibitively high vector dose. To facilitate reduction of vector doses, we improved AAV transduction in skeletal muscle through targeting IR. We did so by introducing an insulin-mimetic peptide, S519, into the AAV capsid, and achieved up to 18-fold enhancement compared to the parental serotypes.

Muscle-tropic vectors have been reported with various transduction efficiencies, including the natural isolates AAV1, AAV2, AAV7, AAV8, and AAV9[51–54] as well as a recently reported serotype isolated from pigs, AAVpo1, that efficiently transduces mouse skeletal

muscle.[55] The engineered vectors AAV2i8 and AAV9.45 preferentially transduce skeletal muscle while detargeting the liver.[56,57] In addition, Paulk et al.[50] recently reported a vector platform for human skeletal muscle transduction based on the directed evolution of natural AAV isolates by genetic shuffling, which yielded NP22 and NP66. Our study shows that the S519 peptide is portable, not only to several natural serotypes, including AAV1, AAV2, and AAV8, but also to NP22. These results suggest that our approach can also be employed in many other AAV vectors, including the next generation vectors that have yet to be designed. In addition to vectors engineered for greater efficiency in certain cell types, a number of novel functional elements are being engineered into AAV capsids, such as protease-activatable "encrypted" vectors[58] and other switchable platforms,[59] in which both high transduction efficiency and specific targeting are pursued. Our approach might prove useful also in combination with these novel elements. Although we chose to use an insulin-mimetic peptide to target IR, owing to our focus on intramuscular delivery, similar strategies can be utilized to target different tissues.

Interestingly, whereas eNP22 and eAAV2 transduce more efficiently than WT NP22 and AAV2 in the skeletal muscle of mice, they do not show any advantage in HEK293T cells. Of note, the receptor-binding regions of NP22 are mostly derived from AAV2,[50] and thus NP22 and AAV2 likely bind heparin sulfate proteoglycan (HSPG) to enter cells. One possible explanation for such a discrepancy is that HSPG is not limiting in HEK293T cells, so that addition of another mode of entry using IR provides no added benefit. In contrast, if HSPG expression is limiting in skeletal muscle, S519-IR interaction would improve the transduction of those vectors. Supporting this idea, differentiated skeletal muscle has a reduced HSPG level compared to undifferentiated myocytes.[60] These data add to a growing body of evidence that *in vitro* studies of AAV transduction are often not predictive of results *in vivo*. Moreover, it underscores the utility of a rational design, like our strategy, that is based on established *in vivo* information, since a mutant with similar phenotype might have been lost in an *in vitro* selection system.

A prior study has shown that insulin could enhance transgene expression.[61] In that study, human factor IX expression in mice was enhanced, albeit modestly (~3-fold), by an insulin pellet subcutaneously implanted before i.m. injection of an AAV1 vector. Although S519, being an IR agonist,[31] could induce similar signaling sequelae as insulin, our data indicate that a majority of eAAVs' superior transduction efficiency comes from its enhanced attachment to the cells through high-affinity S519-IR interaction. Specifically, competitive inhibition of vector binding to cell surface-expressed IR by IR-Fc reduced eAAV9 transduction of 293T cells by >95% at 10 nM (Figure 2E). Further, addition of insulin to cell culture during transduction did not improve the transduction by WT AAV9, but it inhibited transduction by eAAV9 (Figure 2F). Importantly, a reduction of circulating insulin level via fasting enhanced eAAV9-mediated muscle transduction (Figure 4B versus 4C), implying that insulin-mediated signaling is not one of the major mechanisms by which eAAV transduction efficiency was substantially enhanced.

One potential concern for using an insulin-like peptide in gene therapy vectors is that injection of high-titer vectors may induce hypoglycemia. However, a blood glucose measurement study demonstrated this was not the case. While blood glucose was decreased in mice injected with insulin, those injected with eAAV vector at the same dose used for transduction experiments exhibited no significant changes in blood glucose levels compared to the mice injected with WT AAV9 vector. A quick calculation shows that this result is expected. Briefly, at a ratio of 10:1 of WT to mutant capsid, 5–6 copies of the S519 peptide are displayed on each virion, and thus the total peptide copy number per injection of 1×10^9 vg is $5–6 \times 10^9$, or 0.02 pmol. This amount is much lower than the 75 pmol insulin used as a positive control, which is equivalent to a typical human therapeutic dose of 0.5 U/kg for type 2 diabetes mellitus. Even if every one of the 60 copies of capsid on a vector particle were to contain one copy of the S519 peptide, its molar quantity in an injection dose would still be much lower than the therapeutic insulin dose. Moreover, the affinity of the S519 peptide to IR is approximately 40-fold lower than that of insulin.[31] Therefore, even at much higher doses, eAAV would be unlikely to induce hypoglycemia.

One limitation associated with using the S519 peptide is its relatively large size. By modeling binomial distribution of 5–6 mutant capsids on a virion with 20 threefold axes, we estimate that only 25% of threefold axes have one mutant capsid, while 75% have zero mutant capsid. Such low occupancy is likely imposed because steric hindrance would result in defective virus assembly if more than one mutant capsid is present at a given threefold axis. Development of a shorter insulin-mimetic peptide could allow for a higher number of mutant capsids on the virion, thus further enhancing transduction efficiency.

The efficient nature of IR-mediated AAV transduction raises the possibility that a vector could be engineered with fewer native AAV epitopes that are common targets of neutralizing antibodies. These antigenic epitopes map preferentially to regions in the threefold axis.[62] In WT vectors, these regions are not amenable to major modifications because they contain important determinants of cell attachment and entry.[63] However, if efficient cell attachment is provided by an alternative means, a greater degree of change to the native capsid residues could be introduced to avoid neutralizing antibodies without compromising transduction efficiency.

In summary, the results of our study show targeting a receptor highly expressed in a tissue of interest using a high-affinity ligand introduced into an AAV capsid is a strategy of broad utility. This strategy not only substantially enhances AAV vector efficiency, but it also is transferable to other AAV vectors, likely including those that are to be engineered in the future.

MATERIALS AND METHODS

All study procedures were approved by The Scripps Research Institute's Institutional Biosafety Committee, Institutional Review Board,

and Institutional Animal Care and Use Committee, as appropriate. All experiments conform to all relevant regulatory standards.

Plasmid constructs

RepCap expression plasmids for AAV1 and AAV8, deposited by James Wilson (pAAV2/1 and pAAV2/8), and AAV2, deposited by Melina Fan (pAAV2/2), were obtained from Addgene (112862; 112864; 104963). An AAV9 RepCap plasmid was produced by synthesis of the AAV9 Cap gene (GenBank: AX753250.1) and cloning into a pAAV2/5 plasmid (Cell Biolabs) at the HindIII and BshTI sites, replacing the AAV5 capsid gene. Silent mutations were introduced into AAV9 Cap to introduce restriction enzyme sites to facilitate cloning the S519 peptide into VR-IV and VR-VIII. AAV-GFP, a CMV promoter-driven GFP reporter plasmid containing AAV2 inverted terminal repeats (ITRs), deposited by Fred Gage, was obtained from Addgene (49055), and AAV-FLuc plasmid containing AAV2 ITRs was constructed by cloning luc2 (Promega) into the AAV-GFP plasmid. pHelper plasmid that expresses adenovirus E2A, E4, and VA was purchased from Cell Biolabs.

AAV vector production and purification

HEK293T cells were transfected with pHelper plasmid, reporter transgene plasmid, and RepCap plasmid; in the case of eAAV mosaic viruses, the total RepCap plasmid was divided between the mutant and WT RepCap plasmids in the indicated ratio. Cells were lysed by freeze-thaw. Lysates were treated with 50 U/mL Benzonase (Millipore Sigma) and 0.1% Triton X-100 for 1 h at 37°C, then clarified by centrifugation and passed through a 0.45 μm filter. Vectors were captured by AAV-specific affinity resin POROS AAV9 or POROS AAVX (for all other serotypes) in prepacked GoPure columns (Thermo Scientific). Vectors were concentrated in PBS using centrifugal filters with 100 kDa cutoff (Millipore Sigma).

In vivo i.m. transduction

Female BALB/c mice, aged 12 weeks ± 1 week at the time of transduction, were sourced from The Jackson Laboratory. Mice were anesthetized with isoflurane and injected in the medial aspect of the right gastrocnemius muscle with 10^9 vector genomes. Because insulin concentration exhibits diurnal variation,[48,64] mice were injected with vectors in the early afternoon, which is the midpoint of their daily photocycle. Transduction efficiency was assessed at the indicated days post transduction by measuring luciferase activity with RediJect D-Luciferin Bioluminescent Substrate (PerkinElmer) in a Lago X instrument (Spectral Instruments Imaging). To eliminate erroneous measurements from mice that were mishandled by, e.g., suboptimal luciferase substrate injection, mice with luminescence values differing by more than 3-fold from one time point to the next were excluded from analyses.

Detailed descriptions of materials and methods are available in the Supplemental information.

SUPPLEMENTAL INFORMATION

Supplemental Information can be found online at https://doi.org/10.1016/j.omtm.2020.11.004.

ACKNOWLEDGMENTS

We thank Dr. C. Ronald Kahn for the gift of murine brown preadipocyte cells and Joseph Bass for the IR-Fc construct. We also thank Junghae Suh for advice on peptide insertion sites and vector quantification. The Graphical abstract was created with BioRender software. This work was supported by NIH grants R37 AI091476 (to H.C. and M.F.), R44 AI134269 (to M.D.A. and M.F.), and R44 TR003501 (to C.C.B.).

AUTHOR CONTRIBUTIONS

C.B.J., M.F., and H.C. designed research; C.B.J., A.S.R., A.O., K.A.C., and J.M.T. performed research; C.B.J. and H.C. analyzed data; C.C.B., M.D.A., and M.A.K. contributed reagents/analytic tools; C.B.J. and H.C. wrote the paper.

DECLARATION OF INTERESTS

C.B.J., M.F., and H.C. are listed as inventors on a provisional patent for this technology. C.C.B., M.D.A., and M.F. have a financial interest in Emmune, which has licensed the technology from The Scripps Research Institute.

REFERENCES

1. Keeler, A.M., and Flotte, T.R. (2019). Recombinant Adeno-Associated Virus Gene Therapy in Light of Luxturna (and Zolgensma and Glybera): Where Are We, and How Did We Get Here? Annu. Rev. Virol. *6*, 601–621.
2. Ameri, H. (2018). Prospect of retinal gene therapy following commercialization of voretigene neparvovec-rzyl for retinal dystrophy mediated by RPE65 mutation. J. Curr. Ophthalmol. *30*, 1–2.
3. Hoy, S.M. (2019). Onasemnogene Abeparvovec: First Global Approval. Drugs *79*, 1255–1262.
4. George, L.A. (2017). Hemophilia gene therapy comes of age. Blood Adv. *1*, 2591–2599.
5. Batty, P., and Lillicrap, D. (2019). Advances and challenges for hemophilia gene therapy. Hum. Mol. Genet. *28*, R95–R101, R1.
6. Fuchs, S.P., and Desrosiers, R.C. (2016). Promise and problems associated with the use of recombinant AAV for the delivery of anti-HIV antibodies. Mol. Ther. Methods Clin. Dev. *3*, 16068.
7. Martinez-Navio, J.M., Fuchs, S.P., Pedreño-López, S., Rakasz, E.G., Gao, G., and Desrosiers, R.C. (2016). Host Anti-antibody Responses Following Adeno-associated Virus-mediated Delivery of Antibodies Against HIV and SIV in Rhesus Monkeys. Mol. Ther. *24*, 76–86.
8. Julg, B., Liu, P.T., Wagh, K., Fischer, W.M., Abbink, P., Mercado, N.B., Whitney, J.B., Nkolola, J.P., McMahan, K., Tartaglia, L.J., et al. (2017). Protection against a mixed SHIV challenge by a broadly neutralizing antibody cocktail. Sci. Transl. Med. *9*, 9.
9. Barouch, D.H., Whitney, J.B., Moldt, B., Klein, F., Oliveira, T.Y., Liu, J., Stephenson, K.E., Chang, H.W., Shekhar, K., Gupta, S., et al. (2013). Therapeutic efficacy of potent neutralizing HIV-1-specific monoclonal antibodies in SHIV-infected rhesus monkeys. Nature *503*, 224–228.
10. Raper, S.E., and Wilson, J.M. (1995). Gene therapy for human liver disease. Prog. Liver Dis. *13*, 201–230.
11. Cheever, T.R., Berkley, D., Braun, S., Brown, R.H., Byrne, B.J., Chamberlain, J.S., Cwik, V., Duan, D., Federoff, H.J., High, K.A., et al. (2015). Perspectives on best practices for gene therapy programs. Hum. Gene Ther. *26*, 127–133.

12. Wang, L., Bell, P., Somanathan, S., Wang, Q., He, Z., Yu, H., McMenamin, D., Goode, T., Calcedo, R., and Wilson, J.M. (2015). Comparative Study of Liver Gene Transfer With AAV Vectors Based on Natural and Engineered AAV Capsids. Mol. Ther. *23*, 1877–1887.

13. Johnson, P.R., Schnepp, B.C., Zhang, J., Connell, M.J., Greene, S.M., Yuste, E., Desrosiers, R.C., and Clark, K.R. (2009). Vector-mediated gene transfer engenders long-lived neutralizing activity and protection against SIV infection in monkeys. Nat. Med. *15*, 901–906.

14. Mueller, C., Gernoux, G., Gruntman, A.M., Borel, F., Reeves, E.P., Calcedo, R., Rouhani, F.N., Yachnis, A., Humphries, M., Campbell-Thompson, M., et al. (2017). 5 Year Expression and Neutrophil Defect Repair after Gene Therapy in Alpha-1 Antitrypsin Deficiency. Mol. Ther. *25*, 1387–1394.

15. Martinez-Navio, J.M., Fuchs, S.P., Mendes, D.E., Rakasz, E.G., Gao, G., Lifson, J.D., and Desrosiers, R.C. (2020). Long-Term Delivery of an Anti-SIV Monoclonal Antibody With AAV. Front. Immunol. *11*, 449.

16. Greig, J.A., Calcedo, R., Grant, R.L., Peng, H., Medina-Jaszek, C.A., Ahonkhai, O., Qin, Q., Roy, S., Tretiakova, A.P., and Wilson, J.M. (2016). Intramuscular administration of AAV overcomes pre-existing neutralizing antibodies in rhesus macaques. Vaccine *34*, 6323–6329.

17. Keeler, G.D., Markusic, D.M., and Hoffman, B.E. (2019). Liver induced transgene tolerance with AAV vectors. Cell. Immunol. *342*, 103728.

18. Büning, H., Ried, M.U., Perabo, L., Gerner, F.M., Huttner, N.A., Enssle, J., and Hallek, M. (2003). Receptor targeting of adeno-associated virus vectors. Gene Ther. *10*, 1142–1151.

19. Büning, H., and Srivastava, A. (2019). Capsid Modifications for Targeting and Improving the Efficacy of AAV Vectors. Mol. Ther. Methods Clin. Dev. *12*, 248–265.

20. Weinmann, J., and Grimm, D. (2017). Next-generation AAV vectors for clinical use: an ever-accelerating race. Virus Genes *53*, 707–713.

21. Hudry, E., Andres-Mateos, E., Lerner, E.P., Volak, A., Cohen, O., Hyman, B.T., Maguire, C.A., and Vandenberghe, L.H. (2018). Efficient Gene Transfer to the Central Nervous System by Single-Stranded Anc80L65. Mol. Ther. Methods Clin. Dev. *10*, 197–209.

22. Hanlon, K.S., Meltzer, J.C., Buzhdygan, T., Cheng, M.J., Sena-Esteves, M., Bennett, R.E., Sullivan, T.P., Razmpour, R., Gong, Y., Ng, C., et al. (2019). Selection of an Efficient AAV Vector for Robust CNS Transgene Expression. Mol. Ther. Methods Clin. Dev. *15*, 320–332.

23. Davidsson, M., Wang, G., Aldrin-Kirk, P., Cardoso, T., Nolbrant, S., Hartnor, M., Mudannayake, J., Parmar, M., and Björklund, T. (2019). A systematic capsid evolution approach performed in vivo for the design of AAV vectors with tailored properties and tropism. Proc. Natl. Acad. Sci. USA *116*, 27053–27062.

24. Landegger, L.D., Pan, B., Askew, C., Wassmer, S.J., Gluck, S.D., Galvin, A., Taylor, R., Forge, A., Stankovic, K.M., Holt, J.R., and Vandenberghe, L.H. (2017). A synthetic AAV vector enables safe and efficient gene transfer to the mammalian inner ear. Nat. Biotechnol. *35*, 280–284.

25. Carvalho, L.S., Xiao, R., Wassmer, S.J., Langsdorf, A., Zinn, E., Pacouret, S., Shah, S., Comander, J.I., Kim, L.A., Lim, L., and Vandenberghe, L.H. (2018). Synthetic Adeno-Associated Viral Vector Efficiently Targets Mouse and Nonhuman Primate Retina In Vivo. Hum. Gene Ther. *29*, 771–784.

26. Byrne, L.C., Day, T.P., Visel, M., Fortuny, C., Dalkara, D., Merigan, W.H., Schaffer, D.V., and Flannery, J.G. (2020). In vivo directed evolution of AAV in the primate retina. JCI Insight *5*, e135112.

27. Eichhoff, A.M., Börner, K., Albrecht, B., Schäfer, W., Baum, N., Haag, F., Körbelin, J., Trepel, M., Braren, I., Grimm, D., et al. (2019). Nanobody-enhanced targeting of AAV gene therapy vectors. Mol. Ther. Methods Clin. Dev. *15*, 211–220.

28. Ling, C., Li, B., Ma, W., and Srivastava, A. (2016). Development of Optimized AAV Serotype Vectors for High-Efficiency Transduction at Further Reduced Doses. Hum. Gene Ther. Methods *27*, 143–149.

29. Li, M., Jayandharan, G.R., Li, B., Ling, C., Ma, W., Srivastava, A., and Zhong, L. (2010). High-efficiency transduction of fibroblasts and mesenchymal stem cells by tyrosine-mutant AAV2 vectors for their potential use in cellular therapy. Hum. Gene Ther. *21*, 1527–1543.

30. Petrs-Silva, H., Dinculescu, A., Li, Q., Min, S.H., Chiodo, V., Pang, J.J., Zhong, L., Zolotukhin, S., Srivastava, A., Lewin, A.S., and Hauswirth, W.W. (2009). High-efficiency transduction of the mouse retina by tyrosine-mutant AAV serotype vectors. Mol. Ther. *17*, 463–471.

31. Schäffer, L., Brissette, R.E., Spetzler, J.C., Pillutla, R.C., Østergaard, S., Lennick, M., Brandt, J., Fletcher, P.W., Danielsen, G.M., Hsiao, K.-C.C., et al. (2003). Assembly of high-affinity insulin receptor agonists and antagonists from peptide building blocks. Proc. Natl. Acad. Sci. USA *100*, 4435–4439.

32. Naumer, M., Ying, Y., Michelfelder, S., Reuter, A., Trepel, M., Müller, O.J., and Kleinschmidt, J.A. (2012). Development and validation of novel AAV2 random libraries displaying peptides of diverse lengths and at diverse capsid positions. Hum. Gene Ther. *23*, 492–507.

33. Boucas, J., Lux, K., Huber, A., Schievenbusch, S., von Freyend, M.J., Perabo, L., Quadt-Humme, S., Odenthal, M., Hallek, M., and Büning, H. (2009). Engineering adeno-associated virus serotype 2-based targeting vectors using a new insertion site-position 453-and single point mutations. J. Gene Med. *11*, 1103–1113.

34. Judd, J., Wei, F., Nguyen, P.Q., Tartaglia, L.J., Agbandje-McKenna, M., Silberg, J.J., and Suh, J. (2012). Random insertion of mcherry into VP3 domain of adeno-associated virus yields fluorescent capsids with no loss of infectivity. Mol. Ther. Nucleic Acids *1*, e54.

35. Varadi, K., Michelfelder, S., Korff, T., Hecker, M., Trepel, M., Katus, H.A., Kleinschmidt, J.A., and Müller, O.J. (2012). Novel random peptide libraries displayed on AAV serotype 9 for selection of endothelial cell-directed gene transfer vectors. Gene Ther. *19*, 800–809.

36. Michelfelder, S., Varadi, K., Raupp, C., Hunger, A., Körbelin, J., Pahrmann, C., Schrepfer, S., Müller, O.J., Kleinschmidt, J.A., and Trepel, M. (2011). Peptide ligands incorporated into the threefold spike capsid domain to re-direct gene transduction of AAV8 and AAV9 in vivo. PLoS ONE *6*, e23101.

37. Müller, O.J., Kaul, F., Weitzman, M.D., Pasqualini, R., Arap, W., Kleinschmidt, J.A., Trepel, M., Muller, O.J., Kaul, F., Weitzman, M.D., et al. (2003). Random peptide libraries displayed on adeno-associated virus to select for targeted gene therapy vectors. Nat. Biotechnol. *21*, 1040–1046.

38. Edgar, R.C. (2004). MUSCLE: multiple sequence alignment with high accuracy and high throughput. Nucleic Acids Res. *32*, 1792–1797.

39. Waterhouse, A.M., Procter, J.B., Martin, D.M.A., Clamp, M., and Barton, G.J. (2009). Jalview Version 2–a multiple sequence alignment editor and analysis workbench. Bioinformatics *25*, 1189–1191.

40. Goddard, T.D., Huang, C.C., Meng, E.C., Pettersen, E.F., Couch, G.S., Morris, J.H., and Ferrin, T.E. (2018). UCSF ChimeraX: Meeting modern challenges in visualization and analysis. Protein Sci. *27*, 14–25.

41. DiMattia, M.A., Nam, H.-J., Van Vliet, K., Mitchell, M., Bennett, A., Gurda, B.L., McKenna, R., Olson, N.H., Sinkovits, R.S., Potter, M., et al. (2012). Structural insight into the unique properties of adeno-associated virus serotype 9. J. Virol. *86*, 6947–6958.

42. Sanjana, N.E., Shalem, O., and Zhang, F. (2014). Improved vectors and genome-wide libraries for CRISPR screening. Nat. Methods *11*, 783–784.

43. Bass, J., Kurose, T., Pashmforoush, M., and Steiner, D.F. (1996). Fusion of insulin receptor ectodomains to immunoglobulin constant domains reproduces high-affinity insulin binding in vitro. J. Biol. Chem. *271*, 19367–19375.

44. Cao, W., Henry, M.D., Borrow, P., Yamada, H., Elder, J.H., Ravkov, E.V., Nichol, S.T., Compans, R.W., Campbell, K.P., and Oldstone, M.B.A. (1998). Identification of a-dystroglycan as a receptor for lymphocytic choriomeningitis virus and Lassa fever virus. Science *282*, 2079–2081.

45. Pyon, W.S., Gray, D.T., and Barnes, C.A. (2019). An alternative to dye-based approaches to remove background autofluorescence from primate brain tissue. Front. Neuroanat. *13*, 73.

46. Croce, A.C., and Bottiroli, G. (2014). Autofluorescence spectroscopy and imaging: a tool for biomedical research and diagnosis. Eur. J. Histochem. *58*, 2461.

47. Altindis, E., Cai, W., Sakaguchi, M., Zhang, F., GuoXiao, W., Liu, F., De Meyts, P., Gelfanov, V., Pan, H., DiMarchi, R., and Kahn, C.R. (2018). Viral insulin-like peptides activate human insulin and IGF-1 receptor signaling: A paradigm shift for host-microbe interactions. Proc. Natl. Acad. Sci. USA *115*, 2461–2466.

48. Ahrén, B. (2000). Diurnal variation in circulating leptin is dependent on gender, food intake and circulating insulin in mice. Acta Physiol. Scand. *169*, 325–331.

49. Jensen, T.L., Kiersgaard, M.K., Sørensen, D.B., and Mikkelsen, L.F. (2013). Fasting of mice: a review. Lab. Anim. *47*, 225–240.

50. Paulk, N.K., Pekrun, K., Charville, G.W., Maguire-Nguyen, K., Wosczyna, M.N., Xu, J., Zhang, Y., Lisowski, L., Yoo, B., Vilches-Moure, J.G., et al. (2018). Bioengineered Viral Platform for Intramuscular Passive Vaccine Delivery to Human Skeletal Muscle. Mol. Ther. Methods Clin. Dev. *10*, 144–155.

51. Wang, Z., Zhu, T., Qiao, C., Zhou, L., Wang, B., Zhang, J., Chen, C., Li, J., and Xiao, X. (2005). Adeno-associated virus serotype 8 efficiently delivers genes to muscle and heart. Nat. Biotechnol. *23*, 321–328.

52. Lorain, S., Gross, D.A., Goyenvalle, A., Danos, O., Davoust, J., and Garcia, L. (2008). Transient immunomodulation allows repeated injections of AAV1 and correction of muscular dystrophy in multiple muscles. Mol. Ther. *16*, 541–547.

53. Louboutin, J.P., Wang, L., and Wilson, J.M. (2005). Gene transfer into skeletal muscle using novel AAV serotypes. J. Gene Med. *7*, 442–451.

54. Xu, L., Lu, P.J., Wang, C.H., Keramaris, E., Qiao, C., Xiao, B., Blake, D.J., Xiao, X., and Lu, Q.L. (2013). Adeno-associated virus 9 mediated FKRP gene therapy restores functional glycosylation of α-dystroglycan and improves muscle functions. Mol. Ther. *21*, 1832–1840.

55. Tulalamba, W., Weinmann, J., Pham, Q.H., El Andari, J., VandenDriessche, T., Chuah, M.K., and Grimm, D. (2020). Distinct transduction of muscle tissue in mice after systemic delivery of AAVpo1 vectors. Gene Ther. *27*, 170–179.

56. Asokan, A., Conway, J.C., Phillips, J.L., Li, C., Hegge, J., Sinnott, R., Yadav, S., DiPrimio, N., Nam, H.J., Agbandje-McKenna, M., et al. (2010). Reengineering a receptor footprint of adeno-associated virus enables selective and systemic gene transfer to muscle. Nat. Biotechnol. *28*, 79–82.

57. Pulicherla, N., Shen, S., Yadav, S., Debbink, K., Govindasamy, L., Agbandje-McKenna, M., and Asokan, A. (2011). Engineering liver-detargeted AAV9 vectors for cardiac and musculoskeletal gene transfer. Mol. Ther. *19*, 1070–1078.

58. Guenther, C.M., Brun, M.J., Bennett, A.D., Ho, M.L., Chen, W., Zhu, B., Lam, M., Yamagami, M., Kwon, S., Bhattacharya, N., et al. (2019). Protease-Activatable Adeno-Associated Virus Vector for Gene Delivery to Damaged Heart Tissue. Mol. Ther. *27*, 611–622.

59. Katrekar, D., Moreno, A.M., Chen, G., Worlikar, A., and Mali, P. (2018). Oligonucleotide conjugated multi-functional adeno-associated viruses. Sci. Rep. *8*, 3589.

60. Olwin, B.B., and Rapraeger, A. (1992). Repression of myogenic differentiation by aFGF, bFGF, and K-FGF is dependent on cellular heparan sulfate. J. Cell Biol. *118*, 631–639.

61. Carrig, S., Bijjiga, E., Wopat, M.J., and Martino, A.T. (2016). Insulin Therapy Improves Adeno-Associated Virus Transduction of Liver and Skeletal Muscle in Mice and Cultured Cells. Hum. Gene Ther. *27*, 892–905.

62. Tseng, Y.S., and Agbandje-McKenna, M. (2014). Mapping the AAV capsid host antibody response toward the development of second generation gene delivery vectors. Front. Immunol. *5*, 9.

63. Tse, L.V., Klinc, K.A., Madigan, V.J., Castellanos Rivera, R.M., Wells, L.F., Havlik, L.P., Smith, J.K., Agbandje-McKenna, M., and Asokan, A. (2017). Structure-guided evolution of antigenically distinct adeno-associated virus variants for immune evasion. Proc. Natl. Acad. Sci. USA *114*, E4812–E4821.

64. Bailey, C.J., Atkins, T.W., Conner, M.J., Manley, C.G., and Matty, A.J. (1975). Diurnal variations of food consumption, plasma glucose and plasma insulin concentrations in lean and obese hyperglycaemic mice. Horm. Res. *6*, 380–386.